PFC/JA-94-013

Impurity Sources at the First Wall of Alcator C-Mod and their Effect on the Central Plasma

C. Kurz, B. Lipschultz, G.M. McCracken,
M. Graf, J. Snipes, J.L. Terry, B. Welch*

Plasma Fusion Center
Massachusetts Institute of Technology
Cambridge, MA 02139

June 1994

*University of Maryland.

Submitted to Journal of Nuclear Materials

This work was supported by the U. S. Department of Energy Contract No. DE-AC02-78ET51013. Reproduction, translation, publication, use and disposal, in whole or in part by or for the United States government is permitted.

Impurity Sources At The First Wall Of Alcator C-Mod And Their Effect On The Central Plasma

C. Kurz, B. Lipschultz, G. McCracken, M. Graf, J. Snipes, J. Terry, B. Welch

Plasma Fusion Center, MIT, Cambridge, MA 02139, USA

Abstract

In this paper we present data concerning impurity sources and transport in a tokamak with a divertor and molybdenum first wall. A spectrometer, viewing visible and UV light, has been used to take time dependent spectra of C, O, and Mo from both the divertor and the inner limiter surfaces. In the divertor the sputtering threshold for Mo is not normally reached ($T_e \leq 25$ eV). Chord measurements from four filtered photo-diode arrays have enabled us to invert the measured brightness profiles tomographically and obtain 2D emissivity information for H_α and CIII. The total C flux sputtered at the divertor target can be twice as high as from the inner wall surface, increasing with density to about 2×10^{18} s^{-1}. However, modeling the SOL, we find that the penetration efficiency for C is roughly 10 times smaller for the divertor than for the inner wall. Oxygen fluxes are generally observed to be ⅓ of the C flux.

Introduction

The step from a comparatively simple limiter configuration to a complex divertor geometry needs to be justified by a demonstrated improvement in plasma performance. It is universally recognized that among the points in favor of a divertor is its increased capability to retain impurities. At present, a fully 2-D numerical model, which includes multi species impurity transport in the edge as well as in the main plasma, still defeats a practical implementation. An experimental assessment of impurity generation and transport is therefore valuable in furthering our understanding of the divertor and providing input to the divertor design of future machines.

One way of obtaining experimental information about localized impurity generation rates is spectroscopy of visible and near-UV light. Light in this spectral region is usually emitted by low ionization states of light impurities when they are still very close to the point of their origin. The successive transport of these impurity ions and their probability of penetrating the separatrix can be studied either experimentally or numerically.

Experiment

A high density ($\bar{n}_e \approx 2.5\times10^{20}$ m^{-3}), elongated ($\kappa \approx 1.65$) plasma in a closed, single-null divertor geometry with a molybdenum first-wall is typical for present Alcator C-Mod experiments [1,2]. This unique combination of features make Alcator an attractive experiment to study and evaluate regimes of divertor operation relevant to ITER and other future machines.

Emission from the wavelength region between 200 and 1300 nm has been studied with a ½ m grating spectrometer equipped with an MCP image intensifier and a Optical Multichannel Analyzer detector. This instrument

provides a spectral resolution of about 1Å and a time resolution of 30 ms. It has been used to obtain time dependent spectra of C, O, and Mo from both the divertor and the inner limiter surfaces. Several absolutely calibrated Reticon diode arrays, utilizing interference filters to select particular wavelengths of hydrogen and carbon, have been used to obtain spatially resolved emission profiles [2]. The comprehensive coverage of the entire emitting region provided by these arrays has enabled us to invert the measured brightness data tomographically and thus obtain two dimensional emissivity profiles with a spatial resolution of 5 cm. Depending on the brightness of the viewed emission line, the time resolution varies from typically 2 ms for H_α to 16 ms for CIII (4650 Å). A detailed description of the experimental apparatus and the inversion technique will be published in [3] and [4].

Assessment of divertor performance in terms of impurity retention not only requires knowledge of the relevant impurity source strengths and their locations, but also of the screening efficiency of the SOL plasma. This depends on edge plasma parameters such as the electron density and temperature profiles, parallel flow velocity, and connection length. A 1-D impurity transport code, MIST [5], was used to model the SOL and thereby assess its effectiveness in screening the main plasma from impurities. Edge electron temperature and density information for input to the model have been derived from an array of Langmuir probes embedded in the divertor tiles [6].

Carbon Source

Although Alcator uses Mo tiles as first wall material, C present as a contaminant on the tile surface even before installation has been identified as the main source of C.

Using interference filters on two Reticon diode arrays for the 4650 Å CIII multiplet, the combined 128 chordal brightness measurements from the arrays viewing the plasma from the top and the side have been inverted to obtain a local emissivity profile on a 5 cm pixel grid. The emission profile has been interpolated onto a finer grid and smoothed for plotting (see Fig. 1). It can be seen that the emission at the inner wall surface and the outer part of the divertor region dominate, with the upper surfaces of the divertor usually being the brightest source of emission ($\approx$ 200 W m^{-3}).

The MIST code has been used to model edge conditions typical for the wall and the divertor source. To this end we have run MIST for two sets of SOL conditions, representative of the inner wall and the divertor respectively (see Tab. 1). Each SOL condition was then run for two background plasma profiles (corresponding to $\bar{n}_e=1.1\times10^{20}$ m^{-3} and $\bar{n}_e=0.7\times10^{20}$ m^{-3}). Throughout the plasma, $T_i = T_e$ was assumed. The thicker SOL, the shorter connection length, and the faster flow velocity at the divertor all result in an increased probability of the carbon ion to be swept back to the target plate. Given a fixed central carbon density, the required source at the edge to meet that central density has to be 5 times higher at the divertor than at the wall. This number increases with plasma density, an effect also observed by impurity injection experiments [7, 8].

Apart from neutral carbon source rates, MIST also calculates the brightness of the experimentally observed CIII line (λ = 4649 Å). The scaling of the neutral carbon source with the CIII line brightness has been determined for a range of

plasma conditions and is in good agreement with earlier theoretical calculations [9]. This relationship was then used to infer neutral particle fluxes from measured line brightnesses given local plasma temperature and density information. Fig. 2 depicts the experimental data, showing that the divertor carbon source is roughly two times stronger than the wall source. However, the wider SOL and the stronger parallel losses present at the divertor result in a penetration efficiency for carbon which is about 10 times smaller than for the inner wall according to the model. It is the combined effects of source strength and penetration efficiency that determine the contribution of each source to the central impurity content. This leads to the conclusion that the wall source dominates the divertor source by a factor of 3 at moderate densities ($\bar{n}_e \approx 10^{20} m^{-3}$) and gains in importance towards higher densities. Central carbon impurity fractions calculated from the measured source rates and the SOL penetration are around 0.2% of the electron density and agree well with measurements based on UV lines of CVI. These concentrations of C are roughly 1/10 of those observed on machines with a graphite first wall.

Due to the high plasma densities normally achieved in Alcator and the closed divertor geometry, neutral densities in the divertor can reach values of $n_0 \approx 5 \times 10^{19}$ m^{-3} as clculated from H_α radiation. Under these conditions charge exchange enhancement of line emission becomes a concern. For carbon the charge exchange contribution to the total carbon radiation was estimated by MIST runs to be around 20%.

Mo source

Emission lines from MoI and MoII have been observed and identified for views of the inner wall as well as the divertor (for a representative spectrum taken from a view of the divertor that shows two prominent MoI lines see Fig. 3). The plasma conditions under which these measurements have been made were

typically B_T = 5T, I_P = 800 kA, $\bar{n}_e = 8\times10^{19}$ m^{-3}, ohmically heated discharges. Mo fluxes at the inner wall correspond to about 30% of those for carbon. On the other hand, central Mo measurements using a high resolution X-ray spectrometer [10] indicate concentrations of Mo which are about 10% of normal carbon levels. This leads to the conclusion that Mo is better screened in the SOL than carbon.

The situation with respect to Mo sputering is different in the divertor. Lower values of T_e prevent significant sputtering by deuterium. Only during Ar gas puffs in the divertor, when T_e is above a threshold of 8 eV, does the MoI (3902 Å) emission line become clearly visible. Fig. 3 summarizes this observation by plotting the brightness of the MoI (3902 Å) line as a function of divertor electron temperature. The two sets of data correspond to shots with and without Ar gas puffing. The value of the threshold temperature is consistent with physical sputtering by ArII ions. Under the assumption of thermalized ArII, the threshold temperature can be used to determine an effective sheath potential for the divertor target plates (V_s = 2.1 V) using the expression $E_0 = 2T_e^{min} + ZV_s$ for the sputtering threshold energy E_0. Table 2 summarizes the threshold energies and threshold electron temperatures for several different ion species on a Mo target using a value for the sheath potential of V_s = 2.1 V.

Conclusions

We have spectroscopically identified the main impurity species on Alcator C-Mod to be C, O, and Mo. It was found that even though the source rates of C at the divertor are higher than at the wall, the effective screening of impurities by the SOL in the divertor region more than offsets the larger source rate. Hence the carbon density in the plasma is dominated by carbon from the inner wall. Due to the low temperatures prevailing in the divertor, the energy threshold for Mo sputtering by deuterium is not normally reached. Molybdenum has been

observed, however, during Ar gas puffing in the divertor, consistent with the lower energy threshold for sputtering by Ar.

References

[1] I. Hutchinson , R. Boivin, F. Bombarda, Phys. of Plasmas, **1** (1994), 1511

[2] B. Lipschultz, G.M. McCracken, J. Goetz et al., J. Nucl. Matter, this conference

[3] J.L. Terry, J.A. Snipes, J.A. Goetz, C. Kurz, B. Labombard, B. Lipschultz, R. Nachtrieb, Rev. Sci. Instrum., to be published

[4] C. Kurz, J.A. Snipes, J.L. Terry, B. Labombard, B. Lipschultz, G.M. McCracken, Rev. Sci. Instrum., to be published

[5] R.A. Hulse, Nucl. Techn. / Fusion, **3** (1983), 259

[6] B. Labombard, D. Jablonski, B. Lipschultz, G.M. McCracken, J. Goetz, J. Nucl. Matter, this conference

[7] G.M. McCracken, F. Bombarda, M. Graf, J.A. Goetz, D. Jablonski, C. Kurz, B. Labombard, B. Lipschultz, J. Rice, B. Welch, J. Nucl. Matter, this conference

[8] M.A. Graf, J.L. Terry, J.E. Rice, E.S. Marmar, J.A. Goetz, G.M. McCracken, F. Bombarda, M.J. May, Rev. Sci. Instrum., to be published

[9] K. Behringer, H.P. Summers, B. Denne, M. Forrest, M. Stamp, Plasma Phys. Contr. Fus., Vol. 31, No. 14 (1989), 2059

[10] J.E. Rice, F. Bombarda, M.A. Graf, E.S. Marmar, Y. Wang, Rev. Sci, Instrum., to be published

[11] W. Eckstein, J. Bohdansky, J. Roth. Nuc. Fus., **1** (1991), 251

Figure and table captions

Figure 1: Tomographic reconstruction of CIII emission. Also shown is the grid of pixels used in the inversion procedure.

Figure 2: Measured carbon source rates at the inner wall surface and divertor versus line averaged density. The penetration efficiency of carbon across the separatrix is not folded in. (B_T = 5T, I_P = 800 kA, $\bar{n}_e = 10^{20}$ m^{-3})

Figure 3: OMA spectrum taken from a divertor view. Two prominent MoI lines are marked; the majority of lines in this spectrum are from OII and CII.

Figure 4: Brightness of the MoI (3902Å) emission in the divertor. Open symbols are with Ar puffing, full symbols are without Ar puffing.

Table 1: Input parameters to the MIST model of the SOL near the divertor and the inner wall surfaces.

Table 2: Sputtering energy threshold and minimum sputtering electron temperatures for several different ion species on a Mo target [11]. A sheath potential of V_s = 2.1 V has been assumed.

Table 1:

	divertor	inner wall
connection length	2 m	10 m
Mach number	0.3	0.2
SOL thickness	4 cm	2 cm

Table 2:

	E_0 (eV)	T_e^{min} (eV)
H^+	199	49
D^+	90	22
He^+	46	11
He^{2+}	46	7
Ar^+	33	8
Ar^{2+}	33	5

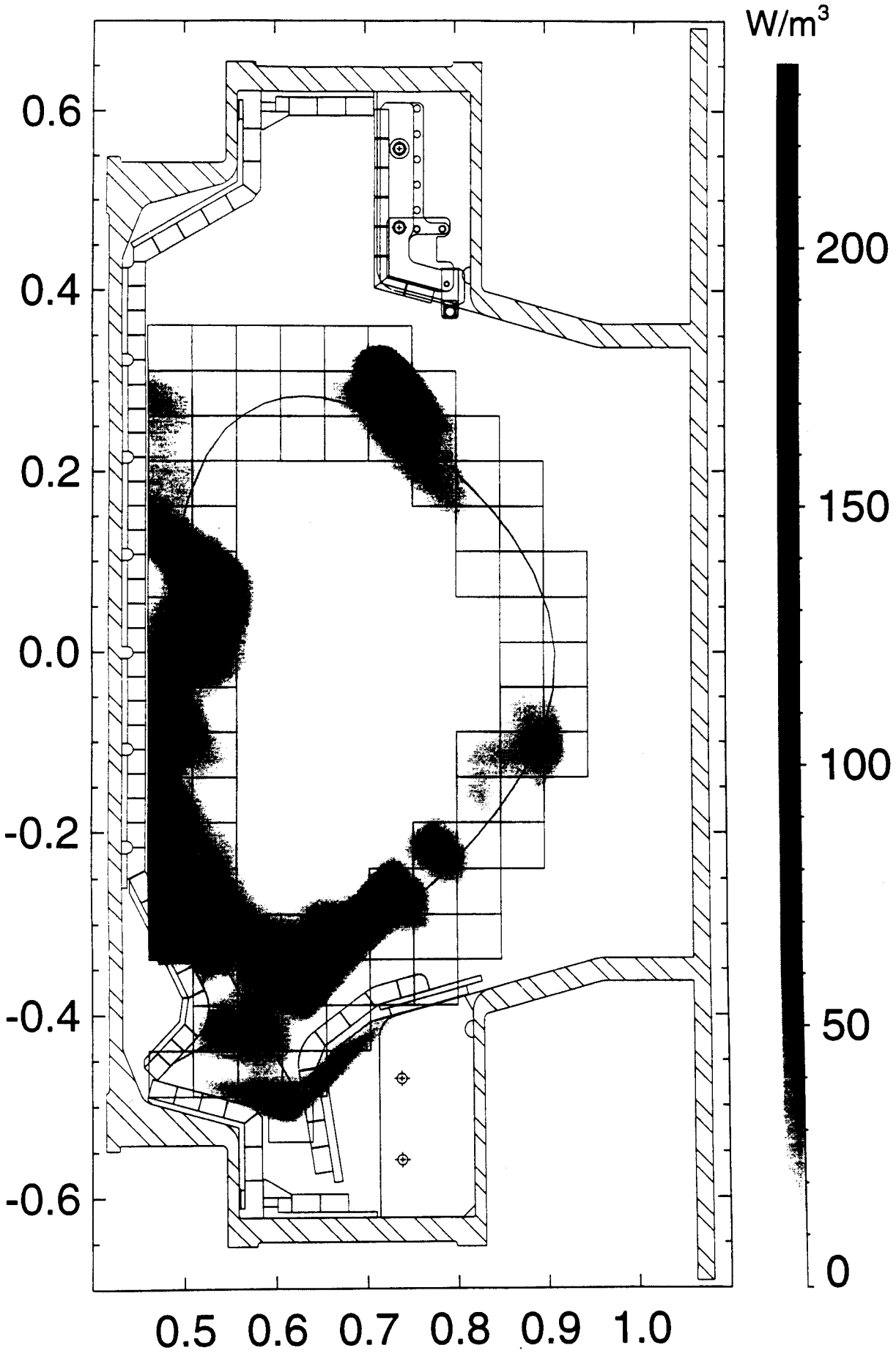

Figure 1

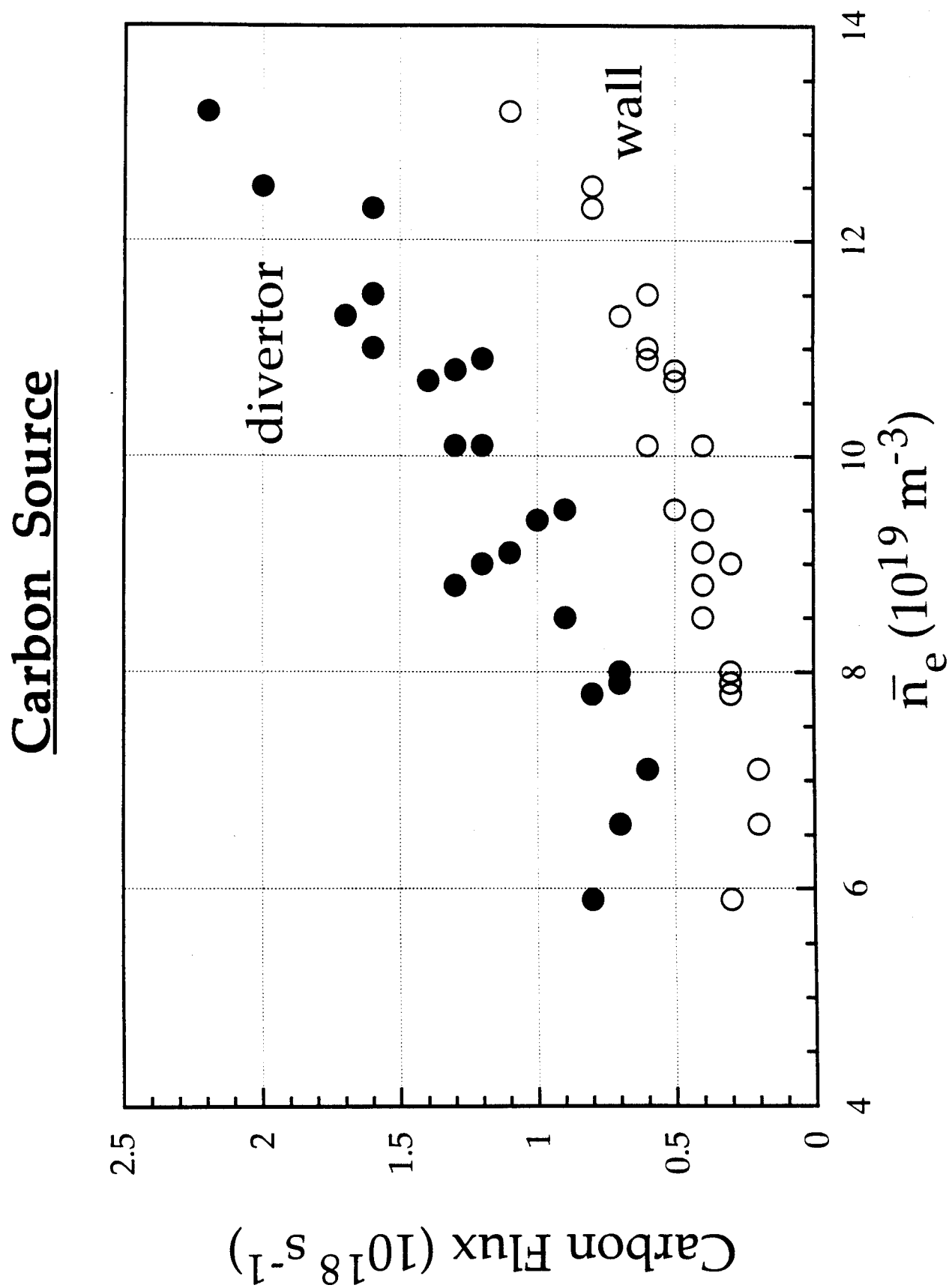
Carbon Source
divertor
wall
Carbon Flux (10^{18} s^{-1})
$\bar{n}_e$ (10^{19} m^{-3})
0
0.5
1
1.5
2
2.5
4
6
8
10
12
14

Figure 2

Divertor Spectrum With Mo Lines

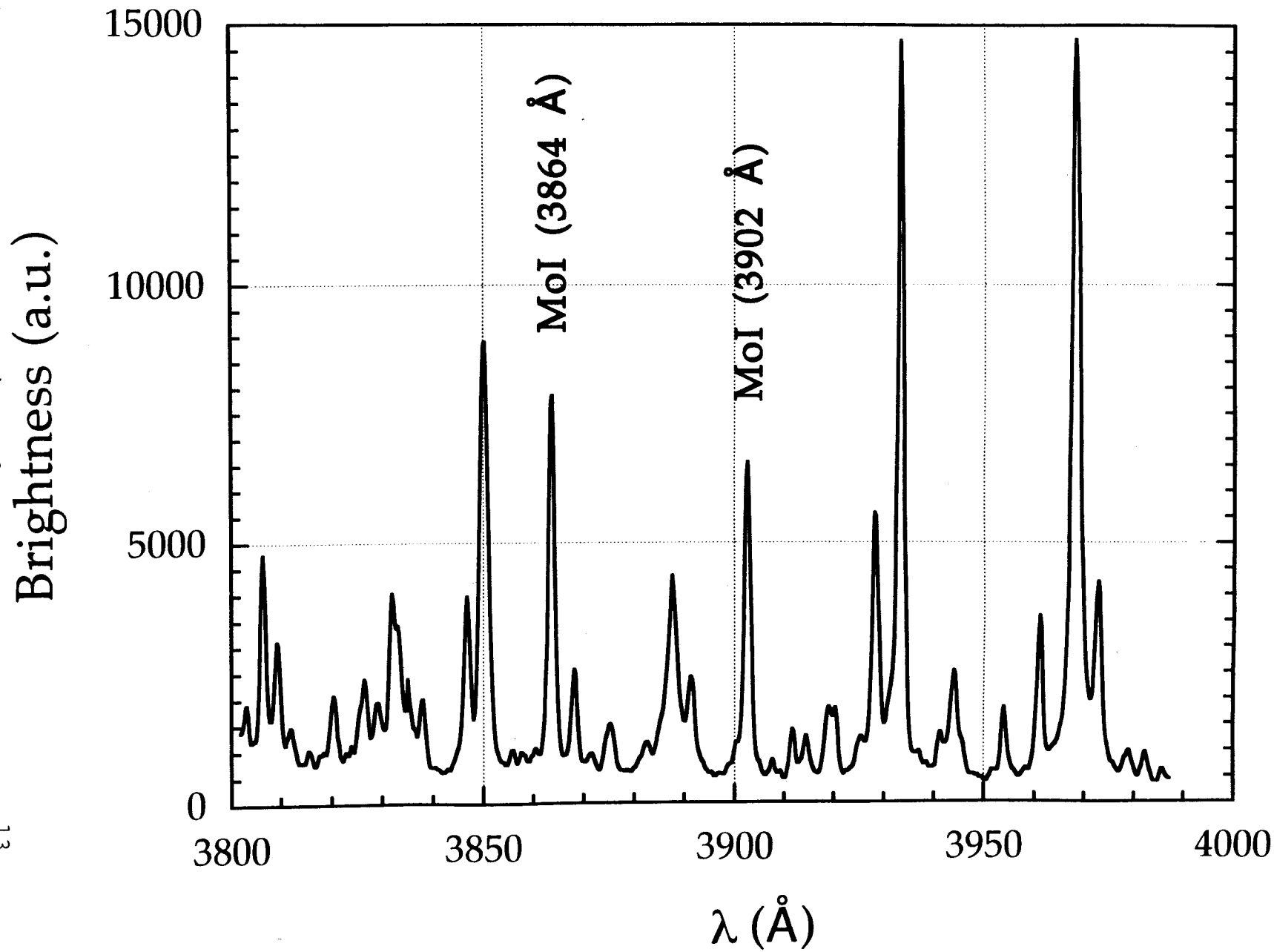

Figure 3

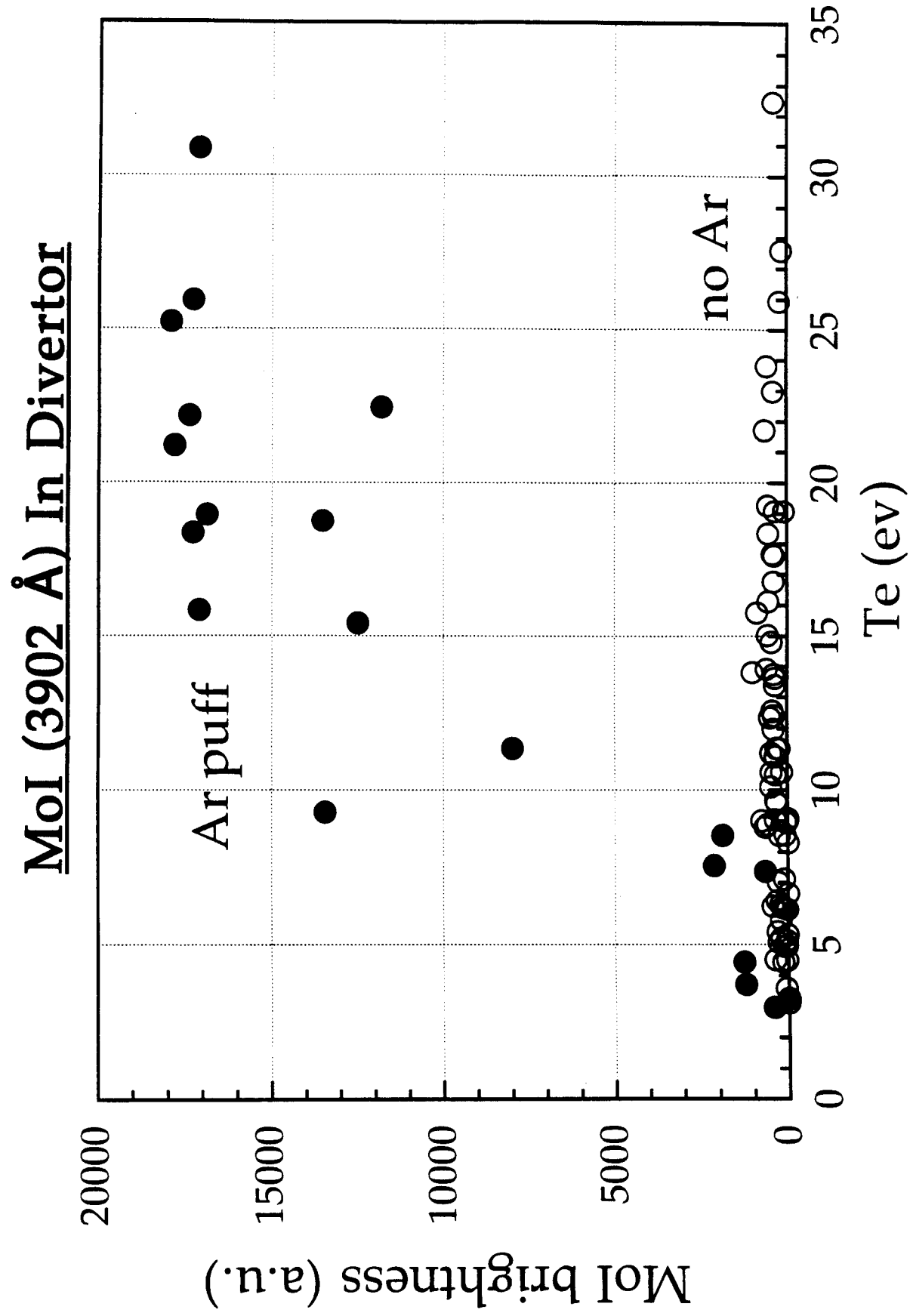
MoI (3902 Å) In Divertor
Ar puff
no Ar
MoI brightness (a.u.)
Te (ev)
0
5000
10000
15000
20000
0
5
10
15
20
25
30
35

Figure 4